Influence of below-cloud evaporation on deuterium excess in precipitation of arid Central Asia and its meteorological controls

Article *in* Journal of Hydrometeorology · July 2016

DOI: 10.1175/JHM-D-15-0203.1

5 authors, including:

Shengjie Wang
The Northwest Normal University

Yanjun Che
The Northwest Normal University

Xiaofan Zhu
Chinese Academy of Sciences

Xuemei Liu
Northeast Institute of Geography and Agroecology Ecology, CAS

Influence of Below-Cloud Evaporation on Deuterium Excess in Precipitation of Arid Central Asia and Its Meteorological Controls

SHENGJIE WANG, MINGJUN ZHANG, YANJUN CHE, XIAOFAN ZHU, AND XUEMEI LIU

College of Geography and Environmental Science, Northwest Normal University, Lanzhou, China

(Manuscript received 21 October 2015, in final form 31 March 2016)

ABSTRACT

The deuterium excess is a second-order parameter linking water-stable oxygen and hydrogen isotopes and has been widely used in hydrological studies. The deuterium excess in precipitation is greatly influenced by below-cloud evaporation through unsaturated air, especially in an arid climate. Based on an observation network of isotopes in precipitation of arid central Asia, the difference in deuterium excess from cloud base to ground was calculated for each sampling site. The difference on the southern slope of the Tian Shan is generally larger than that on the northern slope, and the difference during the summer months is greater than that during the winter months. Generally, an increase of 1% in evaporation of raindrops causes deuterium excess to decrease by approximately 1‰. Under conditions of low air temperature, high relative humidity, heavy precipitation, and large raindrop diameter, a good linear correlation is exhibited between evaporation proportion and difference in deuterium excess, and a linear regression slope of $<1‰\,\%^{-1}$ can be seen; in contrast, under conditions of high air temperature, low relative humidity, light precipitation, and small raindrop diameter, the linear relationship is relatively weak, and the slope is much larger than $1‰\,\%^{-1}$. A sensitivity analysis under different climate scenarios indicates that, if air temperature has increased by 5°C, deuterium excess difference decreases by 0.3‰–4.0‰ for each site; if relative humidity increases by 10%, deuterium excess difference increases by 1.1‰–10.3‰.

1. Introduction

The deuterium excess d (defined as $d = \delta D - 8\delta^{18}O$; Dansgaard 1964) is a second-order isotopic parameter linking stable oxygen and hydrogen isotopes, which is considered as an important tracer in hydrological processes at regional and global scales (e.g., Masson-Delmotte et al. 2005; Aemisegger et al. 2014). The value of d is very sensitive to the meteorological conditions at the point where the vapor was originally evaporated from the surface, including sea surface temperature and relative humidity (Lewis et al. 2013; Benetti et al. 2014; Pfahl and Sodemann 2014; Steen-Larsen et al. 2014). Stable isotopes in falling raindrops are greatly influenced by below-cloud evaporation through unsaturated air especially in arid conditions (Peng et al. 2007; Pang et al. 2011; Ma et al. 2014; Salamalikis et al. 2016). For raindrops falling through ambient air, light isotopes (^{1}H and ^{16}O) are preferentially evaporated, resulting in an enrichment of heavy isotopes (D and ^{18}O) in raindrops as well as a decrease of d.

The quantitative estimation of d variation from cloud base to ground is important in hydrological studies. Based on a laboratory experiment, Stewart (1975) assessed isotope fractionation due to evaporation and isotopic exchange of falling water drops in different gases. The falling water drop model of Stewart (1975) has since been widely used in below-cloud isotope parameterizations of numerical models in which the vertical discretization can be used to account for the vertical gradients and the variability in below-cloud vapor isotope signature, as well as environmental conditions (e.g., temperature and relative humidity) affecting the raindrop–vapor interaction (Zhang et al. 1998; Cappa et al. 2003; Yoshimura et al. 2008). Froehlich et al. (2008) adapted the one-box model of Stewart (1975) and investigated the decrease of d in precipitation from cloud base to ground in the European Alps. A linear correlation between evaporation

Corresponding author address: Mingjun Zhang, College of Geography and Environmental Science, Northwest Normal University, No. 27, Qiujiawan, Anning District, Lanzhou, Gansu 730070, China.
E-mail: mjzhang2004@163.com

DOI: 10.1175/JHM-D-15-0203.1

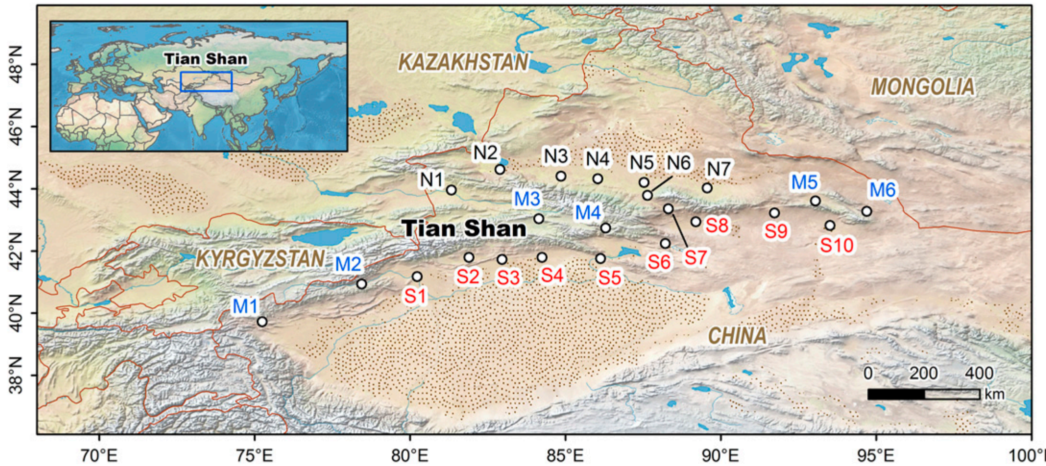

FIG. 1. Map showing the locations of sampling sites in arid central Asia. Northern slope: Yining (N1), Jinghe (N2), Kuytun (N3), Shihezi (N4), Caijiahu (N5), Urumqi (N6), and Qitai (N7). Mountains: Wuqia (M1), Akqi (M2), Bayanbulak (M3), Balguntay (M4), Barkol (M5), and Yiwu (M6). Southern slope: Aksu (S1), Baicheng (S2), Kuqa (S3), Luntai (S4), Korla (S5), Kumux (S6), Dabancheng (S7), Turpan (S8), Shisanjianfang (S9), and Hami (S10). The satellite-derived land cover is acquired from Natural Earth (http://www.naturalearthdata.com), and the distribution of deserts is modified from Wang et al. (2005).

fraction and d in precipitation was reported. A similar method was also applied to other regions (e.g., Kong et al. 2013). However, the input parameters for the one-box Stewart model are generally complex; as a result, many studies directly used the constant linear relationship of approximately 1‰ change per 1% evaporation of raindrop (e.g., Peng et al. 2010; Chen et al. 2015).

In 2012, an observation network of isotopes in precipitation was initiated around the Tian Shan (also known as the Tianshan Mountains) in arid central Asia, and the basic isotopic characteristics in precipitation were discussed by Wang et al. (2016). In an arid and semiarid climate, the isotopic ratios in precipitation are greatly influenced by below-cloud evaporation, and the value of d in precipitation collected at ground may be much different from that in vapor-forming precipitation (Kong et al. 2013; Chen et al. 2015). However, the changes in isotopic composition of falling raindrops in the unsaturated air are still unclear for arid central Asia, and some quantitative assessment based on in situ observation is still needed for regional hydrological studies. To assess the variation of d in precipitation from cloud base to ground, the simple one-box Stewart model was applied to the observation network in this study, and d variations in precipitation for each event were estimated using event-based meteorological parameters. The distribution of d variations is useful to evaluate regional hydrological processes in arid conditions, and to understand the environmental significance of climate proxies (from ice core, speleothem, etc.) in central Asia.

2. Data and method

a. Data and site description

Central Asia lies in the inland of the Eurasian continent, and vast deserts, including the Taklimakan Desert, are located in this region (Fig. 1). The annual mean precipitation is less than 150 mm in arid central Asia (Chen 2012), and westerly vapor advection is the dominant moisture source (Tian et al. 2007; Huang et al. 2015). The Tian Shan is the main mountain range in central Asia, and the precipitation amount in the mountains is much larger than that in surrounding low-lying basins (Zhu et al. 2015). At the eastern portion of the Tian Shan, the annual mean precipitation in mountainous area is 409.1 mm during 1961–2005, which is more than that of the northern (277.3 mm) and southern (66.2 mm) basins (Shi et al. 2008). Precipitation mainly occurs in the summer months from April to October, and precipitation amount in the winter months from November to March (usually snowfall) is very small (Wang et al. 2013).

In 2012, an observation network of stable isotopes in precipitation was established around the Tian Shan. These sampling sites can be classified into three groups: the northern slope (Yining, Jinghe, Kuytun, Shihezi, Caijiahu, Urumqi, and Qitai), the mountains (Wuqia, Akqi, Bayanbulak, Balguntay, Barkol, and Yiwu), and the southern slope (Aksu, Baicheng, Kuqa, Luntai, Korla, Kumux, Dabancheng, Turpan, Shisanjianfang, and Hami). From August 2012 to September 2013, there were 1052 event-based precipitation samples collected at 23 stations in this observation network. The seasonal variation and meteorological controls of stable isotopes in precipitation were presented by Wang et al. (2016). The focus of this study is on the influence of below-cloud evaporation on d in precipitation.

The sampling was undertaken by the full-time meteorological observers at these stations. To prevent evaporation, liquid samples were collected immediately after the end of the rain event and transferred to 60-mL high-density polyethylene (HDPE) bottles with waterproof seals. Solid samples were melted at room temperature in low-density polyethylene (LDPE) bags before being stored in bottles. The precipitation amount for each event was manually measured by the meteorological observers. Air temperature, vapor pressure, and relative humidity during precipitation were recorded on an hourly basis by automatic weather stations and then were arithmetically averaged for each event. The precipitation samples were analyzed for stable hydrogen and oxygen isotopes using a liquid water isotope analyzer DLT-100 (Los Gatos Research, Inc.) at the Stable Isotope Laboratory, College of Geography and Environmental Science, Northwest Normal University. Every sample and isotopic standard was injected sequentially six times, with the first two injections discarded because of memory effects, and the results were expressed as δ values relative to Vienna Standard Mean Ocean Water (VSMOW). The measurement precision is ±0.6‰ for δD and ±0.2‰ for δ^{18}O. More information on sampling and sample analysis is given in Wang et al. (2016).

b. Method

Influenced by below-cloud evaporation of raindrops, the stable isotopic ratios in collected precipitation near ground may be considerably different from that below the cloud base. The changes of hydrogen and oxygen isotope ratios and d in raindrops from cloud base to ground (values at ground minus values at cloud base) can be expressed as

$$\Delta^2\delta = {}^2\delta_{\mathrm{gr}} - {}^2\delta_{\mathrm{cb}}, \tag{1a}$$

$$\Delta^{18}\delta = {}^{18}\delta_{\mathrm{gr}} - {}^{18}\delta_{\mathrm{cb}}, \quad \text{and} \tag{1b}$$

$$\Delta d = d_{\mathrm{gr}} - d_{\mathrm{cb}}, \tag{1c}$$

where ${}^2\delta_{\mathrm{gr}}$ (${}^{18}\delta_{\mathrm{gr}}$) and ${}^2\delta_{\mathrm{cb}}$ (${}^{18}\delta_{\mathrm{cb}}$) are the hydrogen (oxygen) isotope compositions of a falling raindrop near ground and below cloud base, respectively, and d_{gr} and d_{cb} are d values of a raindrop near ground and below cloud base, respectively.

According to Stewart (1975), the isotopic composition of a falling water drop is

$${}^2R_{\mathrm{gr}} = {}^2\gamma{}^2R_{\mathrm{va}} + ({}^2R_{\mathrm{cb}} - {}^2\gamma{}^2R_{\mathrm{va}})f^{{}^2\beta} \quad \text{and} \tag{2a}$$

$${}^{18}R_{\mathrm{gr}} = {}^{18}\gamma{}^{18}R_{\mathrm{va}} + ({}^{18}R_{\mathrm{cb}} - {}^{18}\gamma{}^{18}R_{\mathrm{va}})f^{{}^{18}\beta}, \tag{2b}$$

where ${}^2R_{\mathrm{gr}}$ (${}^{18}R_{\mathrm{gr}}$), ${}^2R_{\mathrm{va}}$ (${}^{18}R_{\mathrm{va}}$), and ${}^2R_{\mathrm{cb}}$ (${}^{18}R_{\mathrm{cb}}$) are hydrogen (oxygen) isotopic ratios of a falling raindrop near ground, vapor at cloud base, and raindrop at cloud base, respectively; f is the remaining fraction of raindrop mass after evaporation; and the parameters of ${}^2\gamma$, ${}^{18}\gamma$, ${}^2\beta$, and ${}^{18}\beta$ (Stewart 1975) are defined as

$${}^2\gamma = \frac{{}^2\alpha h}{1 - {}^2\alpha({}^2D/{}^2D')^k(1-h)}, \tag{3a}$$

$${}^{18}\gamma = \frac{{}^{18}\alpha h}{1 - {}^{18}\alpha({}^{18}D/{}^{18}D')^k(1-h)}, \tag{3b}$$

$${}^2\beta = \frac{1 - {}^2\alpha({}^2D/{}^2D')^k(1-h)}{{}^2\alpha({}^2D/{}^2D')^k(1-h)}, \quad \text{and} \tag{3c}$$

$${}^{18}\beta = \frac{1 - {}^{18}\alpha({}^{18}D/{}^{18}D')^k(1-h)}{{}^{18}\alpha({}^{18}D/{}^{18}D')^k(1-h)}, \tag{3d}$$

where ${}^2\alpha$ and ${}^{18}\alpha$ are equilibrium fractionation factors for hydrogen and oxygen isotopes, respectively (Friedman and O'Neil 1977; Criss 1999); h is relative humidity; ${}^2D/{}^2D'$ and ${}^{18}D/{}^{18}D'$ are 1.024 and 1.0289, respectively (Merlivat 1970; Stewart 1975); and k is 0.58.

If below-cloud precipitation and surrounding ambient water vapor are assumed to be in isotopic equilibrium, Froehlich et al. (2008) determined the value of Δd caused by below-cloud evaporation as

$$\Delta d = \left(1 - \frac{{}^2\gamma}{{}^2\alpha}\right)(f^{{}^2\beta} - 1) - 8\left(1 - \frac{{}^{18}\gamma}{{}^{18}\alpha}\right)(f^{{}^{18}\beta} - 1), \tag{4a}$$

and the values of $\Delta^2\delta$ and $\Delta^{18}\delta$ [also see Salamalikis et al. (2016)] are

$$\Delta^2\delta = \left(1 - \frac{{}^2\gamma}{{}^2\alpha}\right)(f^{{}^2\beta} - 1) \quad \text{and} \tag{4b}$$

$$\Delta^{18}\delta = \left(1 - \frac{{}^{18}\gamma}{{}^{18}\alpha}\right)(f^{{}^{18}\beta} - 1). \tag{4c}$$

The raindrop is usually assumed as a spheroid (Kinzer and Gunn 1951), and the remaining fraction of raindrop mass can be calculated as

$$f = \frac{m_{\mathrm{end}}}{m_{\mathrm{end}} + m_{\mathrm{ev}}}, \tag{5}$$

where m_{end} is the mass of the raindrop touching ground and m_{ev} is evaporated mass of raindrop and is defined as

$$m_{\mathrm{ev}} = Et, \tag{6}$$

where E is evaporation intensity (evaporated water mass per unit time) and t is time of falling drop from

TABLE 1. Comparison of d in precipitation at ground and cloud base for each sampling site around the Tian Shan from August 2012 to September 2013. The values of d at ground are taken from Wang et al. (2016).

	Annual				Summer months				Winter months			
	d (‰)				d (‰)				d (‰)			
Site	Ground	Cloud base	Δd	n	Ground	Cloud base	Δd	n	Ground	Cloud base	Δd	n
Northern slope												
Yining (N1)	8.8	12.5	−3.6	90	9.6	16.1	−6.5	58	7.9	7.9	0.0	32
Jinghe (N2)	3.2	16.4	−13.3	42	3.4	16.8	−13.4	40	−12.6	−12.6	0.0	2
Kuytun (N3)	10.9	19.5	−8.6	47	12.1	22.3	−10.2	38	4.3	4.3	0.0	9
Shihezi (N4)	12.5	20.4	−7.8	74	10.9	22.2	−11.3	55	16.2	16.2	0.0	19
Caijiahu (N5)	10.9	17.4	−6.5	58	10.6	19.1	−8.5	35	11.6	11.9	−0.3	23
Urumqi (N6)	16.6	18.3	−1.7	75	19.7	22.1	−2.3	41	9.1	9.1	0.0	34
Qitai (N7)	16.0	20.1	−4.1	44	17.5	22.4	−4.9	29	9.4	9.8	−0.4	15
Mountains												
Wuqia (M1)	14.4	24.9	−10.5	65	14.4	25.4	−11.0	61	14.4	14.4	0.0	4
Akqi (M2)	11.2	17.4	−6.2	62	11.2	17.6	−6.4	59	11.1	11.1	0.0	3
Bayanbulak (M3)	14.3	24.2	−9.9	96	14.6	24.9	−10.2	87	6.4	6.4	0.0	9
Balguntay (M4)	10.3	14.2	−3.9	60	10.3	14.2	−3.9	60	—	—	—	0
Barkol (M5)	9.4	14.5	−5.1	53	9.9	15.7	−5.8	34	5.9	6.3	−0.5	19
Yiwu (M6)	10.7	22.1	−11.4	23	10.2	21.9	−11.7	21	28.8	28.8	0.0	2
Southern slope												
Aksu (S1)	9.2	23.5	−14.3	39	9.3	23.9	−14.6	35	3.5	3.5	0.0	4
Baicheng (S2)	5.9	22.5	−16.6	52	6.3	23.9	−17.6	45	−1.0	−1.0	0.0	7
Kuqa (S3)	7.2	25.1	−17.8	40	6.6	26.9	−20.3	35	11.8	11.8	0.0	5
Luntai (S4)	10.6	22.6	−12.0	25	11.1	24.8	−13.7	24	7.1	7.1	0.0	1
Korla (S5)	2.6	24.1	−21.5	22	1.4	25.8	−24.3	16	11.8	11.8	0.0	6
Kumux (S6)	5.2	23.0	−17.8	28	5.5	26.6	−21.1	24	3.6	3.6	0.0	4
Dabancheng (S7)	13.6	19.8	−6.3	12	13.5	20.0	−6.4	11	14.3	14.3	0.0	1
Turpan (S8)	−8.6	10.0	−18.7	21	−14.4	17.5	−31.9	17	−0.5	−0.5	0.0	4
Shisanjianfang (S9)	−4.9	30.4	−35.3	6	−5.3	34.1	−39.4	4	−1.4	−1.4	0.0	2
Hami (S10)	4.9	13.3	−8.4	18	−2.9	17.8	−20.7	9	10.2	10.2	0.0	9

cloud base to ground. The falling raindrop is considered to be in constant motion, and the falling time is

$$t = \frac{H_{cb}}{v_{end}}, \qquad (7)$$

where H_{cb} is height of cloud base and v_{end} is terminal velocity of raindrop.

Based on Kinzer and Gunn (1951), raindrop evaporation intensity is a product of functions Q_1 and Q_2:

$$E = Q_1(T, D)Q_2(T, h), \qquad (8)$$

where Q_1 is a function (cm) of ambient air temperature T and raindrop diameter D, and Q_2 is a function (g cm^{-1} s^{-1}) of air temperature and relative humidity. The values of Q_1 and Q_2 for specific conditions (i.e., $T = 0°, 10°, 20°, 30°, 40°$C; $D = 0.01, 0.02, 0.03, \ldots, 0.44$ cm; and $h = 10\%, 20\%, 30\%, \ldots, 100\%$) were presented by Kinzer and Gunn (1951). To acquire Q_1 and Q_2 at specific meteorological conditions for each precipitation event in this study, a bilinear interpolation method was used.

The terminal velocity can be calculated using Best (1950a):

$$v_{end} = \begin{cases} 9.58e^{0.0354H_{cb}}[1 - e^{-(D/1.77)^{1.147}}], & 0.3 \le D < 6.0 \\ 1.88e^{0.0256H_{cb}}[1 - e^{-(D/0.304)^{1.819}}], & 0.05 \le D < 0.3, \\ 28.40D^2e^{0.0172H_{cb}}, & D < 0.05 \end{cases} \qquad (9)$$

where v_{end} is terminal velocity of raindrop (m s^{-1}), e is natural constant, H_{cb} is height at cloud base (km), and D is diameter of raindrop (mm).

The cloud-base height is determined as lifting condensation level (LCL) in this study (Wang et al. 2009; Fletcher and Bretherton 2010; Yang et al. 2014) and can be calculated using a barometric formula (von Herrmann 1906):

$$H_{cb} = 18\,400\left(1 + \frac{T_{mean}}{273}\right)\lg\frac{S_0}{S_{LCL}}, \qquad (10)$$

where T_{mean} is average air temperature (°C) between LCL and surface, S_0 is measured pressure (hPa) at surface, and S_{LCL} is pressure (hPa) at LCL (Barnes 1968) and is defined as

$$S_{LCL} = S_0\left(\frac{T_{LCL}}{T_0}\right)^{3.5}, \qquad (11)$$

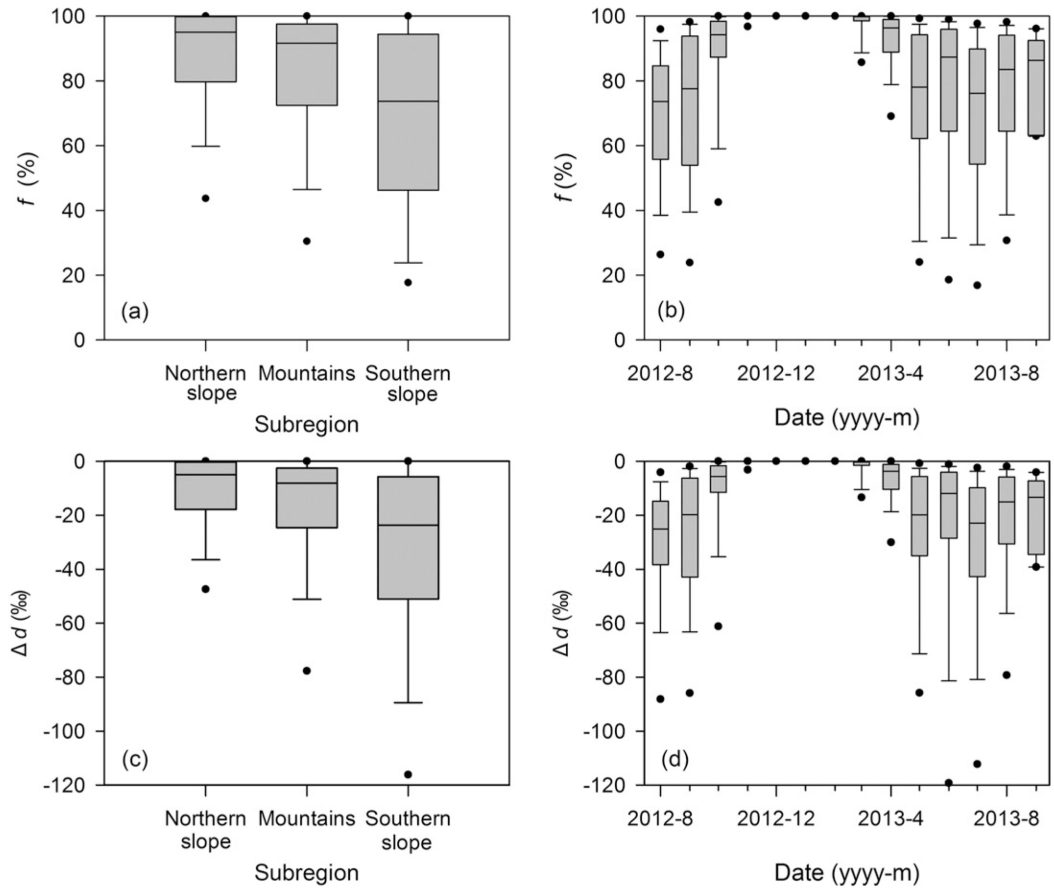

FIG. 2. Regional and monthly variation of (a),(b) f and (c),(d) Δd in precipitation around the Tian Shan from August 2012 to September 2013. Boxes represent the 25%–75% percentiles, and the line through the box represents the median (50th percentile). Whiskers indicate the 90th and 10th percentiles, and points above and below the whiskers indicate the 95th and 5th percentiles.

where S_0 is pressure at the observation site (hPa) and T_{LCL} and T_0 are air temperature (K) at LCL and at the surface. Air temperature at LCL is calculated using an empirical formula (Barnes 1968):

$$T_{LCL} = T_{dp_0} - (0.001\,296 T_{dp_0} + 0.1963)(T_0 - T_{dp_0}), \tag{12}$$

where T_{dp_0} and T_0 are the dewpoint and air temperature (°C) at the observation sites. The accuracy of Eqs. (11) and (12) was discussed in Barnes (1968).

It should be mentioned that Eqs. (10)–(12) are only applied to estimate the cloud-base height and then the falling time of raindrop, which does not change the basic assumption of homogeneous condition in the one-box approach. In some previous studies on isotopic modeling of below-cloud evaporation effect in precipitation, the 850-hPa heights (~1500 m) were used as cloud-base heights (e.g., Kong et al. 2013; Salamalikis et al. 2016). In this observation network around the Tian Shan, many sampling stations are higher than 1500 m MSL (surface pressure <850 hPa), so an LCL-based cloud-base height was applied to calculate the falling distance of raindrops.

The raindrop size distribution is not a routine observation for meteorological stations in the study region (Li et al. 2003) and was estimated using precipitation intensity in this study. Best (1950b) presented an empirical formula on raindrop size distribution:

$$1 - F = e^{-(D/AI^q)^c}, \tag{13}$$

where F is fraction of liquid water in the air composed of raindrops with diameter less than D; e is natural constant; I is precipitation intensity (mm h^{-1}); and the parameters of c, A, and q are 2.25, 1.30, and 0.232, respectively. If $F = 0.5$, the median diameter of the raindrops is

$$D_{50} = \sqrt[c]{0.69} A I^q. \tag{14}$$

3. Result and discussion

a. Basic pattern

Table 1 shows the average values of d at ground (from Wang et al. 2016) and cloud base for each sampling site around the Tian Shan in arid central Asia. On an annual basis, Δd varies from −35.3‰ (Shisanjianfang) to −1.7‰ (Urumqi), and the arithmetic mean is −11.4‰. During the summer months (from April to October), Δd ranges between −39.4‰ and −2.3‰, and the arithmetic mean is −13.7‰; during the winter months (from November to March), the range is from −0.5‰ to 0‰, and the arithmetic mean is −0.1‰. Generally, the difference in d between the ground and the cloud base in the summer months is greater than during the winter months.

Compared with the measured d in precipitation, the estimated d at cloud base shows more spatial coherence at some sites. For example, Kuytun, Shihezi, Urumqi, and Qitai are located on the northern slope of the Tian Shan, and the measured d values in precipitation during the summer months range from 10.9‰ (Shihezi) to 19.7‰ (Urumqi). The estimated d at cloud base is very similar for all these sites, and the values range between 22.1‰ (Urumqi) and 22.4‰ (Qitai). This indicates that these sites may have similar moisture sources, and the spatial pattern is greatly influenced by below-cloud evaporation (maybe also by surface evaporation and transpiration). In an arid climate, the impact of subcloud evaporation on stable isotopic ratios in precipitation samples should be considered in hydrological studies.

The model used in this study originates from laboratory work undertaken by Stewart (1975), who formulated a still widely used empirical model on the heavy isotope mass exchange rate between a raindrop and the surrounding vapor. In this study, the model is applied in a one-box approach as it was in Froehlich et al. (2008), in which the conditions are homogeneous and the cloud vapor isotope ratios are assumed to be equal to the below-cloud vapor isotope ratios. The assumption of homogeneous air column may influence the results, because the air temperature, relative humidity, and vapor isotopic compositions logically vary in atmosphere. More observation of vapor isotopes and vertical meteorological variation may be helpful to improve the results (Aemisegger et al. 2012). However, as demonstrated in Salamalikis et al. (2016), the one-box model is still of significance to assess the subcloud evaporation effect.

In the recent years, the influence of subcloud evaporation on precipitation isotopes on an intraevent time scale has been widely investigated (e.g., Lee and Fung 2008; Risi et al. 2010; Yoshimura et al. 2010; Aemisegger et al. 2015). In attempting to model the isotopic composition of precipitation for a winter storm in the western United States, Yoshimura et al. (2010) found that kinetic isotopic exchange between falling raindrops and ambient air needed to be considered. In a central European example, Aemisegger et al. (2015) found that neglecting below-cloud processes resulted in modeled vapor isotopes being more depleted than observations by 20‰–40‰ for δD and 5‰–10‰ for δ^{18}O. Our study agrees with these previous studies in finding that the short-time-scale isotopic composition in precipitation is influenced by subcloud processes.

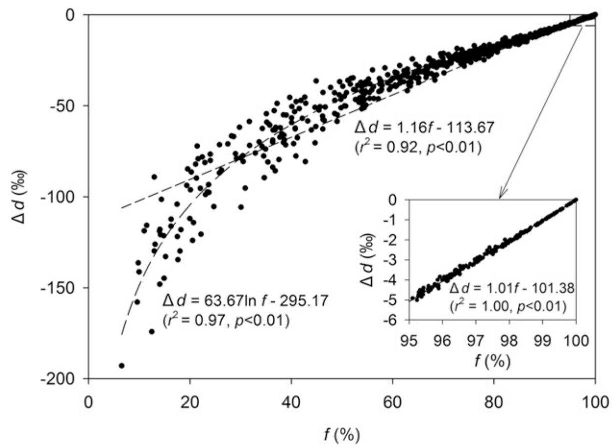

FIG. 3. Relationship between f and Δd in precipitation around the Tian Shan from August 2012 to September 2013.

b. Raindrop evaporation and Δd

As shown in Figs. 2a and 2b, the remaining fraction of raindrop mass varies depending on location and season. According to the median value, the remaining fraction on the southern slope is much less than that on the northern slope and in the mountains. The value of f on the northern slope and mountains is generally larger than 80% [also the case in Froehlich et al. (2008)], and that on the southern slope is less than 70%. In the summer months, especially from June to September, as air temperature increases, evaporation intensity increases and the remaining fraction decreases. During the winter months, surface air temperature is usually less than 0°C and almost all the precipitation samples are solid, that is, precipitation falls as snow. The drop evaporation during winter is negligible and the remaining fraction is close to 100%. In the summer months under high air temperature conditions, the raindrop strongly evaporates when falling through the air and the remaining fraction is very low in some sites, especially on the southern slope. Figures 2c and 2d illustrate the variation of Δd in precipitation for the study region,

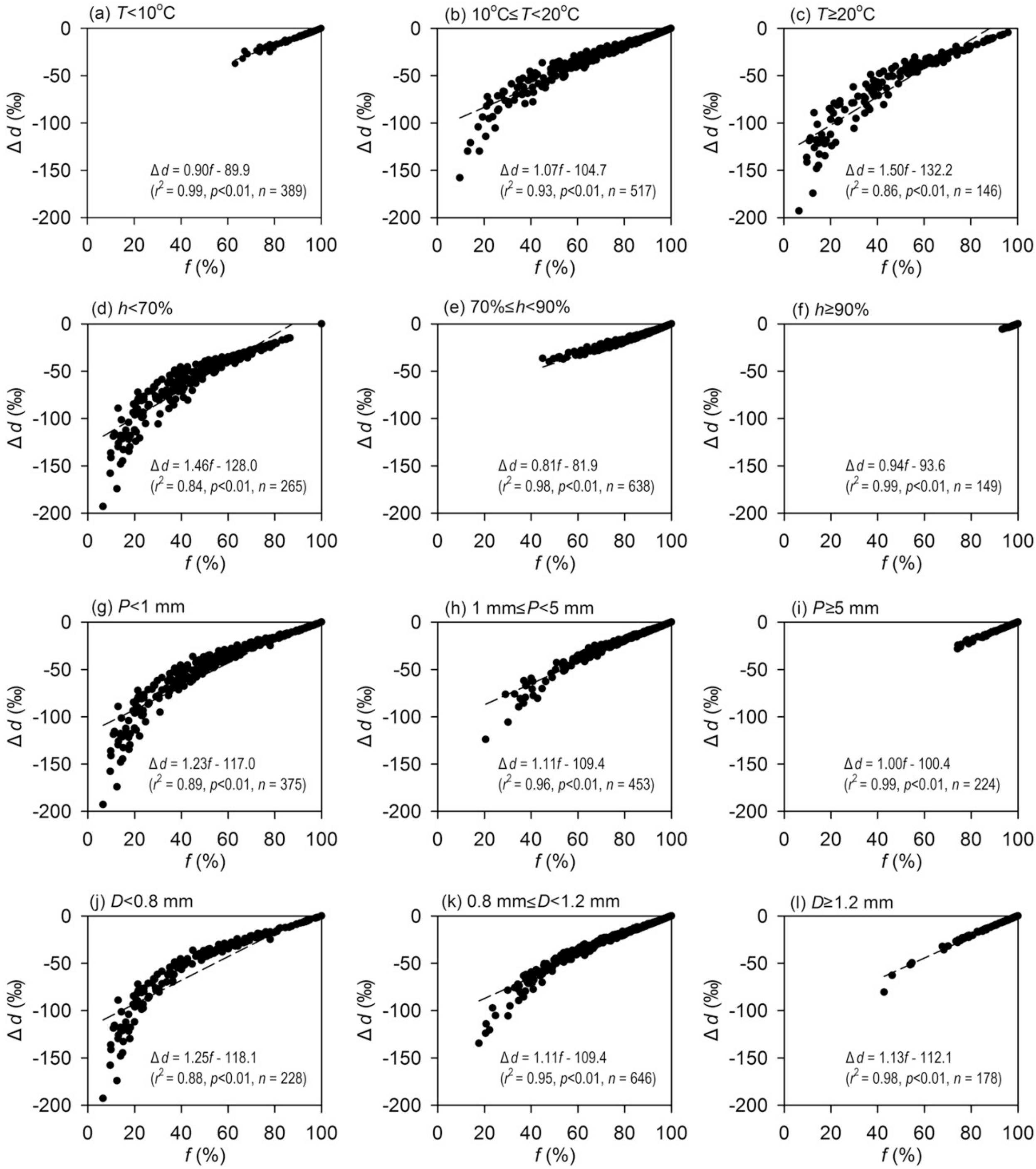

FIG. 4. Relationship between f and Δd in precipitation for different meteorological conditions [air temperature (i.e., T), relative humidity (i.e., h), precipitation amount (i.e., P), and raindrop diameter (i.e., D)] around the Tian Shan from August 2012 to September 2013.

showing that the seasonal and spatial patterns are similar to those for f.

It is clear that Δd is related to remaining fraction, and Fig. 3 shows the correlations between the two parameters. As mentioned in previous studies (Froehlich et al. 2008; Kong et al. 2013), under a condition of high remaining fraction (usually >95%), there is good linear relationship between f and Δd with a slope ($\Delta d/f$) of approximately 1‰ $\%^{-1}$ (1.1‰ $\%^{-1}$ or 1.2‰ $\%^{-1}$), which means that a 1% increase of evaporation may

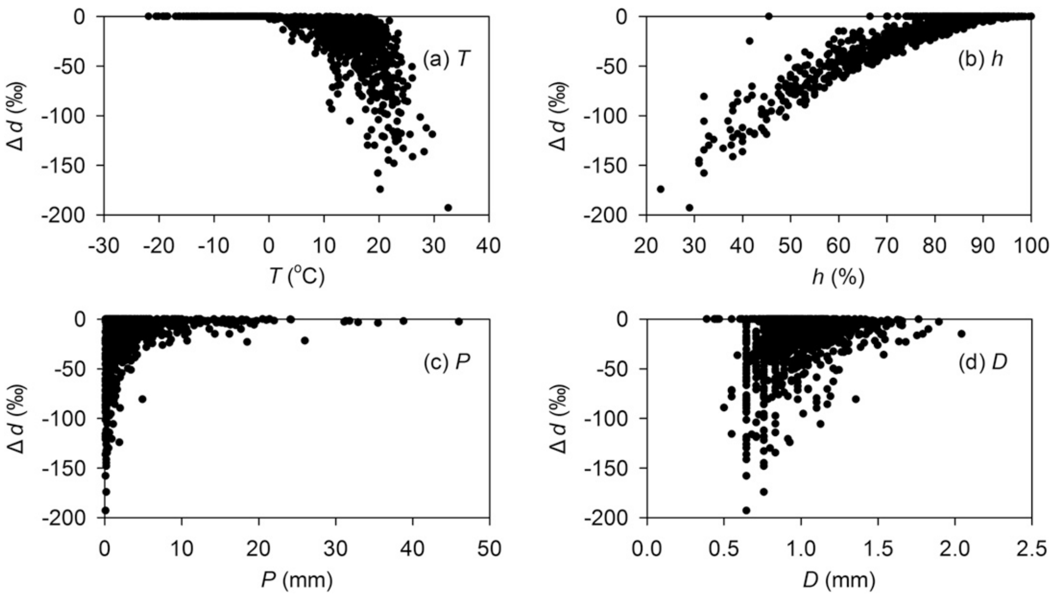

FIG. 5. Relationship between meteorological parameters (T, h, P, and D) and Δd in precipitation around the Tian Shan from August 2012 to September 2013.

cause d to decrease by approximately 1‰. In an arid climate, the remaining fraction of raindrop mass may be much less than 95%, and almost all the mass may disappear for small raindrops (Mason and Ramanadham 1954; Salamalikis et al. 2016).

Considering a subset of remaining fraction larger than 95%, a good linear relationship (approximately 1‰ $\%^{-1}$) is seen from the inset in Fig. 3. Under a condition of high remaining fraction, the mass loss of raindrop through the air is small, and the relationship between f and Δd is linear. The relationship gradually becomes weaker as the remaining fraction decreases. When the remaining fraction decreases to 20% (although this is not very frequent), the scattering around the regression line becomes stronger. In some studies (Peng et al. 2010; Chen et al. 2015), the regression slope of approximately 1‰ $\%^{-1}$ acquired from the European Alps has been directly applied to other regions to quantify below-cloud evaporation using the measured d in precipitation at neighboring sites. In a wet and cold region with high remaining fraction, the empirical regression (1‰ $\%^{-1}$) may be applicable. However, in arid and semiarid climates, the linear relationship should be treated with caution.

c. Meteorological controls

The relationship between the remaining fraction and Δd is associated with meteorological conditions such as air temperature and relative humidity (Fig. 4). Generally, under a condition of low air temperature, high relative humidity, large precipitation amount, and big raindrop diameter, the remaining fraction is large and Δd is close to 0; the linear correlation between the remaining fraction and Δd is observed; and the slope of the regression line between Δd and the remaining fraction is slightly lower, which means that a 1% increase of evaporation corresponds to Δd variations of less than 1‰. In contrast, in an arid environment with high air temperature, low relative humidity, small precipitation amount, and small raindrop diameter, the remaining fraction is relatively small and the difference in Δd is large; the relationship between the two parameters is not linear, and the slope is usually larger than 1‰ $\%^{-1}$. Below 0°C, the precipitation is usually snowfall, and the subcloud evaporation through the air is generally ignorable (Fig. 5a). As air temperature increases, Δd greatly departs from 0. With increasing relative humidity, Δd becomes closer to 0, but the variation of Δd is very limited when relative humidity is higher than 90% (Fig. 5b). Where precipitation amount is small, Δd has a wide range from 0 to approximately −200‰ (Fig. 5c). As precipitation amount increases, the value of Δd tends toward 0. In addition, when raindrop diameter is large, Δd is generally close to 0 (Fig. 5d). Among the four parameters, relative humidity generally exerts the main control on the obtained Δd.

A sensitivity test of Δd under different scenarios for air temperature and relative humidity is exhibited in Fig. 6. During the sampling period, air temperature for each event ranges from −21.9° to 32.6°C, with an arithmetic mean of 10.2°C. For the liquid samples only, the arithmetic mean of air temperature is 14.8°C. Relative

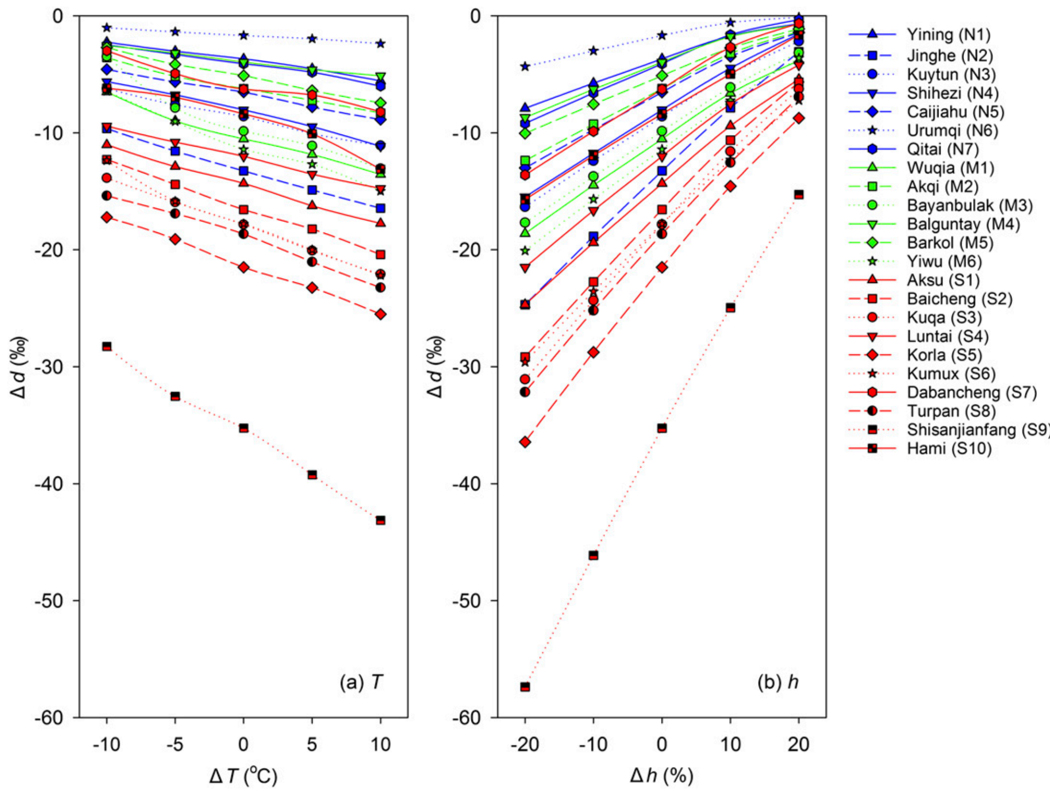

FIG. 6. Variation of Δd in precipitation for each sampling site around the Tian Shan under different (a) T and (b) h conditions. Sampling sites for the three subregions are marked in different colors, that is, the northern slope (blue), the mountains (green), and the southern slope (red).

humidity ranges between 23% and 100% with an arithmetic mean of 76.8%, while the arithmetic mean for all the liquid samples is 74.1%. Using a step width of 5°C, four climate scenarios of air temperature variation (decreasing or increasing by 5° and 10°C) were calculated (Fig. 6a); four scenarios of relative humidity variation from decreasing by 20% to increasing by 20% were also shown in Fig. 6b. If air temperature would increase by 5°C at all the sampling sites, Δd would decrease by 0.3‰–4.0‰ (arithmetic mean over all sites is 1.5‰), and the values for each subregion are 0.3‰–1.6‰ on the northern slope, 0.7‰–1.3‰ in the mountains, and 0.5‰–4.0‰ on the southern slope, respectively. If relative humidity increases by 10%, Δd increases by 1.1‰–10.3‰ (arithmetic mean is 4.3‰), and the decreases for each subregion are 1.1‰–5.4‰, 2.2‰–4.2‰, and 3.4‰–10.3‰, respectively.

The in situ observation of raindrop size distribution over the Tian Shan is very limited. To our knowledge, the only report was at two alpine sites in June and July 2001 (Li et al. 2003). In that study, the raindrop diameter was usually less than 1 mm, but the rare raindrops of diameter >3 mm may greatly contribute to precipitation intensity. Besides that measurement, there is no investigation of the spatial pattern of raindrop size for different underlying surfaces around the Tian Shan. According to the probability distribution function of precipitation intensity in China (Sun 2004), there may be great spatial dependency and seasonal variation in precipitation intensity as well as raindrop diameter around the Tian Shan. Because of the limited measurement availability, the diameters are usually set as a constant in the one-box Stewart model. For instance, the input diameter is 2.6 mm in the European Alps (Froehlich et al. 2008) and 0.74 mm in the eastern Tian Shan (Kong et al. 2013). A diameter-constant setting for a large domain may significantly influence the estimation accuracy. Using a step width of 0.2 mm, the values of Δd are recalculated with constant diameter from 0.3 to 4.4 mm at each sampling site (Fig. 7). It is clear that the influence of raindrop diameter on Δd in precipitation cannot be ignored. If the raindrop diameter is larger than 2 mm, the change of d is always less than 10‰ (except at Shisanjianfang). If the raindrop diameter is smaller than 1 mm, values of Δd smaller than −30‰ can be seen at many sampling sites, even at the mountainous sites.

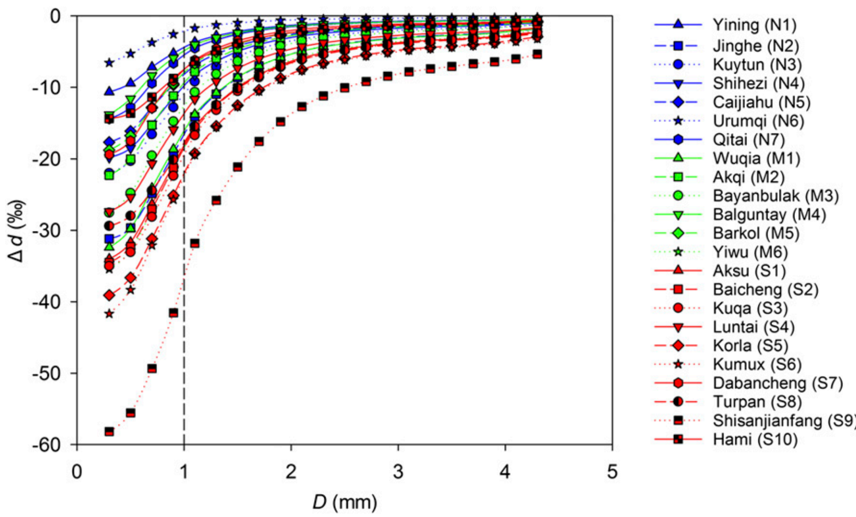

FIG. 7. Relationship between D and Δd in precipitation for each sampling site around the Tian Shan. Sampling sites for the three subregions are marked in different colors, that is, the northern slope (blue), the mountains (green), and the southern slope (red). The vertical dashed line denotes the mean diameter in this study (1.0 mm).

4. Conclusions

Stable isotopic ratios in precipitation are influenced by below-cloud evaporation. In this study, a simple one-box Stewart model was applied to assess the variation in d of raindrops from cloud base to ground. The difference in d (Δd) from cloud base to ground varies, depending on location. The difference on the southern slope is larger than that on the northern slope, and Δd during the summer months is larger than that during the winter months. A linear relationship is seen between the remaining fraction of the raindrop mass and Δd ($r^2 = 0.92$, $p < 0.01$). As raindrop mass evaporation increases by 1%, d in precipitation decreases by approximately 1‰. Under conditions of low air temperature, high relative humidity, large precipitation amount, and raindrop diameter, the change in d below the cloud is small, and the relationship between the remaining fraction and Δd is linear. Under conditions of high air temperature, low relative humidity, small precipitation amount, and diameter, Δd is relatively large, and the correlation coefficient between the remaining fraction and Δd is relatively small. The sensitivity analysis under different climate scenarios indicates that, if air temperature has increased by 5°C, Δd in precipitation decreases by 0.3‰–4.0‰ for each site in the study region; if relative humidity increases by 10%, Δd increases by 1.1‰–10.3‰. Although the model conditions are homogeneous and the cloud vapor isotope ratios are assumed to be equal to the below-cloud vapor isotope ratios, the simulated changes of d in raindrop generally reflect the regional climate background, which is consistent with previous studies on an intraevent time scale.

Acknowledgments. This study is funded by the National Natural Science Foundation of China (Awards 41161012 and 41240001) and the National Basic Research Program of China (Award 2013CBA01801). The authors greatly thank all the meteorological stations in the observation network for providing the meteorological parameters, and the colleagues at Northwest Normal University for data processing. The authors also thank Yanlong Kong (Chinese Academy of Sciences), Jagoda Crawford, and Catherine Hughes (Australian Nuclear Science and Technology Organisation) for their warm help and useful suggestions.

REFERENCES

Aemisegger, F., P. Sturm, P. Graf, H. Sodemann, S. Pfahl, A. Knohl, and H. Wernli, 2012: Measuring variations of $\delta^{18}O$ and δ^2H in atmospheric water vapour using two commercial laser-based spectrometers: An instrument characterisation study. *Atmos. Meas. Tech.*, **5**, 1491–1511, doi:10.5194/amt-5-1491-2012.

——, S. Pfahl, H. Sodemann, I. Lehner, S. I. Seneviratne, and H. Wernli, 2014: Deuterium excess as a proxy for continental moisture recycling and plant transpiration. *Atmos. Chem. Phys.*, **14**, 4029–4054, doi:10.5194/acp-14-4029-2014.

——, J. Spiegel, S. Pfahl, H. Sodemann, W. Eugster, and H. Wernli, 2015: Isotope meteorology of cold front passages: A case study combining observations and modeling. *Geophys. Res. Lett.*, **42**, 5652–5660, doi:10.1002/2015GL063988.

Barnes, S. L., 1968: An empirical shortcut to the calculation of temperature and pressure at the lifted condensation level. *J. Appl. Meteor.*, **7**, 511, doi:10.1175/1520-0450(1968)007<0511:AESTTC>2.0.CO;2.

Benetti, M., G. Reverdin, C. Pierre, L. Merlivat, C. Risi, H. C. Steen-Larsen, and F. Vimeux, 2014: Deuterium excess in marine water vapor: Dependency on relative humidity and surface wind speed during evaporation. *J. Geophys. Res. Atmos.*, **119**, 584–593, doi:10.1002/2013JD020535.

Best, A. C., 1950a: Empirical formulae for the terminal velocity of water drops falling through the atmosphere. *Quart. J. Roy. Meteor. Soc.*, **76**, 302–311, doi:10.1002/qj.49707632905.

——, 1950b: The size distribution of raindrops. *Quart. J. Roy. Meteor. Soc.*, **76**, 16–36, doi:10.1002/qj.49707632704.

Cappa, C. D., M. B. Hendricks, D. J. DePaolo, and R. C. Cohen, 2003: Isotopic fractionation of water during evaporation. *J. Geophys. Res.*, **108**, 4525, doi:10.1029/2003JD003597.

Chen, F., M. Zhang, S. Wang, Q. Ma, X. Zhu, and L. Dong, 2015: Relationship between sub-cloud secondary evaporation and stable isotope in precipitation of Lanzhou and surrounding area. *Quat. Int.*, **380–381**, 68–74, doi:10.1016/j.quaint.2014.12.051.

Chen, X., 2012: *Retrieval and Analysis of Evapotranspiration in Central Areas of Asia* (in Chinese). China Meteorological Press, 214 pp.

Criss, R. E., 1999: *Principles of Stable Isotope Distribution*. Oxford University, 264 pp.

Dansgaard, W., 1964: Stable isotopes in precipitation. *Tellus*, **16**, 436–468, doi:10.1111/j.2153-3490.1964.tb00181.x.

Fletcher, J. K., and C. S. Bretherton, 2010: Evaluating boundary layer-based mass flux closures using cloud-resolving model simulations of deep convection. *J. Atmos. Sci.*, **67**, 2212–2225, doi:10.1175/2010JAS3328.1.

Friedman, I., and J. R. O'Neil, 1977: Compilation of stable isotope fractionation factors of geochemical interest. *Data of Geochemistry*, 6th ed. M. Fleischer, Ed., Geological Survey Professional Paper 440-KK, USGS, 117 pp.

Froehlich, K., M. Kralik, W. Papesch, D. Rank, H. Scheifinger, and W. Stichler, 2008: Deuterium excess in precipitation of Alpine regions—Moisture recycling. *Isotopes Environ. Health Stud.*, **44**, 61–70, doi:10.1080/10256010801887208.

Huang, W., J. Chen, X. Zhang, S. Feng, and F. Chen, 2015: Definition of the core zone of the "westerlies-dominated climatic regime," and its controlling factors during the instrumental period. *Sci. China Earth Sci.*, **58**, 676–684, doi:10.1007/s11430-015-5057-y.

Kinzer, G. D., and R. Gunn, 1951: The evaporation, temperature and thermal relaxation-time of freely falling waterdrops. *J. Meteor.*, **8**, 71–83, doi:10.1175/1520-0469(1951)008<0071:TETATR>2.0.CO;2.

Kong, Y., Z. Pang, and K. Froehlich, 2013: Quantifying recycled moisture fraction in precipitation of an arid region using deuterium excess. *Tellus*, **65B**, 19251, doi:10.3402/tellusb.v65i0.19251.

Lee, J. E., and I. Fung, 2008: "Amount effect" of water isotopes and quantitative analysis of post-condensation processes. *Hydrol. Processes*, **22**, 1–8, doi:10.1002/hyp.6637.

Lewis, S. C., A. N. LeGrande, M. Kelley, and G. A. Schmidt, 2013: Modeling insights into deuterium excess as an indicator of water vapor source conditions. *J. Geophys. Res. Atmos.*, **118**, 243–262, doi:10.1029/2012JD017804.

Li, Y., B. Du, and X. Zhou, 2003: Features of raindrop size distributions in Tianshan area (in Chinese with English abstract). *J. Nanjing Inst. Meteor.*, **26**, 465–472.

Ma, Q., M. Zhang, S. Wang, Q. Wang, W. Liu, F. Li, and F. Chen, 2014: An investigation of moisture sources and secondary evaporation in Lanzhou, Northwest China. *Environ. Earth Sci.*, **71**, 3375–3385, doi:10.1007/s12665-013-2728-x.

Mason, B. J., and R. Ramanadham, 1954: Modification of the size distribution of falling raindrops by coalescence. *Quart. J. Roy. Meteor. Soc.*, **80**, 388–394, doi:10.1002/qj.49708034508.

Masson-Delmotte, V., and Coauthors, 2005: GRIP deuterium excess reveals rapid and orbital-scale changes in Greenland moisture origin. *Science*, **309**, 118–121, doi:10.1126/science.1108575.

Merlivat, L., 1970: Quantitative aspects of the study of water balances in lakes using the deuterium and oxygen-18 concentrations in the water. *Proc. Isotope Hydrology 1970 Symp.*, Vienna, Austria, IAEA, 89–107. [Available online at https://inis.iaea.org/search/search.aspx?orig_q=RN:38054521.]

Pang, Z., Y. Kong, K. Froehlich, T. Huang, L. Yuan, Z. Li, and F. Wang, 2011: Processes affecting isotopes in precipitation of an arid region. *Tellus*, **63B**, 352–359, doi:10.1111/j.1600-0889.2011.00532.x.

Peng, H., B. Mayer, S. Harris, and H. Krouse, 2007: The influence of below-cloud secondary effects on the stable isotope composition of hydrogen and oxygen in precipitation at Calgary, Alberta, Canada. *Tellus*, **59B**, 698–704, doi:10.1111/j.1600-0889.2007.00291.x.

Peng, T.-R., C.-H. Wang, C.-C. Huang, L.-Y. Fei, C.-T. A. Chen, and J.-L. Hwong, 2010: Stable isotopic characteristic of Taiwan's precipitation: A case study of western Pacific monsoon region. *Earth Planet. Sci. Lett.*, **289**, 357–366, doi:10.1016/j.epsl.2009.11.024.

Pfahl, S., and H. Sodemann, 2014: What controls deuterium excess in global precipitation? *Climate Past*, **10**, 771–781, doi:10.5194/cp-10-771-2014.

Risi, C., S. Bony, F. Vimeux, M. Chong, and L. Descroix, 2010: Evolution of the stable water isotopic composition of the rain sampled along Sahelian squall lines. *Quart. J. Roy. Meteor. Soc.*, **136**, 227–242, doi:10.1002/qj.485.

Salamalikis, V., A. A. Argiriou, and E. Dotsika, 2016: Isotopic modeling of the sub-cloud evaporation effect in precipitation. *Sci. Total Environ.*, **544**, 1059–1072, doi:10.1016/j.scitotenv.2015.11.072.

Shi, Y., Z. Sun, and Q. Yang, 2008: Characteristics of area precipitation in Xinjiang region with its variations (in Chinese with English abstract). *J. Appl. Meteor. Sci.*, **19**, 326–332.

Steen-Larsen, H. C., and Coauthors, 2014: Climatic controls on water vapor deuterium excess in the marine boundary layer of the North Atlantic based on 500 days of in situ, continuous measurements. *Atmos. Chem. Phys.*, **14**, 7741–7756, doi:10.5194/acp-14-7741-2014.

Stewart, M. K., 1975: Stable isotope fractionation due to evaporation and isotopic exchange of falling water drops: Applications to atmospheric processes and evaporation of lakes. *J. Geophys. Res.*, **80**, 1133–1146, doi:10.1029/JC080i009p01133.

Sun, X., 2004: *Precipitation Intensity Distribution and Rainfall Attenuation in Ku Band in Major Cities in China* (in Chinese). China Meteorological Press, 192 pp.

Tian, L., T. Yao, K. MacClune, J. W. C. White, A. Schilla, B. Vaughn, R. Vachon, and K. Ichiyanagi, 2007: Stable isotopic variations in west China: A consideration of moisture sources. *J. Geophys. Res.*, **112**, D10112, doi:10.1029/2006JD007718.

von Herrmann, C. F., 1906: Problems in meteorology. *Mon. Wea. Rev.*, **34**, 574–579, doi:10.1175/1520-0493(1906)34<574:PIM>2.0.CO;2.

Wang, J., and Coauthors, 2009: Impact of deforestation in the Amazon basin on cloud climatology. *Proc. Natl. Acad. Sci. USA*, **106**, 3670–3674, doi:10.1073/pnas.0810156106.

Wang, S., M. Zhang, M. Sun, B. Wang, and X. Li, 2013: Changes in precipitation extremes in alpine areas of the Chinese Tianshan Mountains, central Asia, 1961–2011. *Quat. Int.*, **311**, 97–107, doi:10.1016/j.quaint.2013.07.008.

——, ——, C. E. Hughes, X. Zhu, L. Dong, Z. Ren, and F. Chen, 2016: Factors controlling stable isotope composition of precipitation in arid conditions: An observation network in the Tianshan Mountains, central Asia. *Tellus.*, **68B**, 26206, doi:10.3402/tellusb.v68.26206.

Wang, Y., J. Wang, Y. Qi, and C. Yan, 2005: Dataset of desert distribution in China (1:100,000). Environmental and Ecological Science Data Center for West China, National Natural Science Foundation of China, accessed 1 June 2014, doi:10.3972/westdc.006.2013.db.

Yang, Y.-M., I.-S. Kang, and M. Almazroui, 2014: A mass flux closure function in a GCM based on the Richardson number. *Climate Dyn.*, **42**, 1129–1138, doi:10.1007/s00382-014-2079-7.

Yoshimura, K., M. Kanamitsu, D. Noone, and T. Oki, 2008: Historical isotope simulation using reanalysis atmospheric data. *J. Geophys. Res.*, **113**, D19108, doi:10.1029/2008JD010074.

——, ——, and M. Dettinger, 2010: Regional downscaling for stable water isotopes: A case study of an atmospheric river event. *J. Geophys. Res.*, **115**, D18114, doi:10.1029/2010JD014032.

Zhang, X., Z. Xie, and T. Yao, 1998: Mathematical modeling of variations on stable isotopic ratios in falling raindrops. *Acta Meteorol. Sin.*, **12**, 213–220.

Zhu, X., M. Zhang, S. Wang, F. Qiang, T. Zeng, Z. Ren, and L. Dong, 2015: Comparison of monthly precipitation derived from high-resolution gridded datasets in arid Xinjiang, central Asia. *Quat. Int.*, **358**, 160–170, doi:10.1016/j.quaint.2014.12.027.